# Spectroscopic Analysis of Models for Heme $d_1$: Isomeric Copper(II) Porphyrindiones

**Muthusamy Mylrajan,[1a,b] Laura A. Andersson,*[,1c] Thomas M. Loehr,[1a] Weishih Wu,[1d] and Chi K. Chang[1d]**

*Contribution from the Department of Chemical and Biological Sciences, Oregon Graduate Institute of Science and Technology, Beaverton, Oregon 97006-1999, Department of Biochemistry, Willard Hall, Kansas State University, Manhattan, Kansas 66506, and Department of Chemistry, Michigan State University, East Lansing, Michigan 48824.*
*Received December 7, 1990*

**Abstract:** The heme $d_1$ prosthetic group of bacterial dissimilatory nitrite reductases is an iron 1,3-bis(carbomethoxymethyl)-7-(carbomethoxyethenyl)-6-(carbomethoxyethyl)-1,3,5,8-tetramethyl-2,4-dioxoporphyrin. To model this unusual macrocycle, we have examined a variety of copper(II)-metalated 2,4- and 2,3-dioxoporphyrins (diones). Peripheral substituents were changed systematically to investigate conjugated and nonconjugated substituent effects; $^{15}N_4$- and meso-$d_4$-substituted isomers of 2,4- and 2,3-octaethylporphyrindiones were also studied. Generalized spectral properties of diones include an increase in the resonance Raman (RR) and Fourier transform infrared (FTIR) spectral complexity relative to the case of the porphyrins and the presence of a cluster of bands in the 1330–1420-cm$^{-1}$ region of the RR spectra. These features, a consequence of the low effective symmetry of diones, are similar to those of chlorins. However, because of the 45° rotation of the $C_2$ symmetry axis for diones, their RR polarization properties are distinct from those of chlorins. Overall spectral properties of diones are dominated by the conjugated oxo substituents. Carbonyl region FTIR spectra of diones are perturbed by nonconjugated peripheral substituents. The normal-mode composition of dioxoporphyrins differs from those of porphyrins and chlorins, as exemplified by both $^{15}N_4$ and meso-$d_4$ sensitivity of bands in the ~1330–1420-cm$^{-1}$ region of the RR spectra. The strong, polarized RR band at 1340–1350 cm$^{-1}$ and the ~1710-cm$^{-1}$ $\nu$(C=O) feature(s) appear to be diagnostic for dione macrocycles, as distinct from porphyrins, chlorins, or isobacteriochlorins. Although the spectra of heme $d_1$ and the analogous dione models are very similar, every structural change away from the substituent pattern of the in vivo $d_1$ macrocycle decreases the correspondence. This work will aid in the analysis of structure/function correlations for dissimilatory nitrite reductases.

## Introduction

Cytochrome $cd_1$ is a multiheme dissimilatory nitrite reductase found in many denitrifying bacteria, including *Pseudomonas aeruginosa*,[2] *Paracoccus denitrificans*,[3] *Alcaligenes faecalis*,[4] and *Thiobacillus denitrificans*.[5] These enzymes are produced anaerobically, and in the presence of nitrite function as nitrite reductases.[6] In the absence of nitrite, cytochrome $cd_1$ also functions as a cytochrome oxidase, reducing $O_2$ to $H_2O$.[7]

Native cytochrome $cd_1$ is composed of two identical subunits of $M_r$ ~60000. Each subunit contains one heme $c$ covalently bonded to the polypeptide and one noncovalently associated heme $d_1$.[8] A chlorin structure with 10 substituents was originally proposed for the $d_1$ macrocycle on the basis of spectroscopic data.[9] However, Chang[10] subsequently suggested that heme $d_1$ was a 2,4-substituted dioxoporphyrin (dione[11]) with an acrylate substituent (structure **1** in Figure 1). This macrocyclic structure for heme $d_1$ is strongly supported by optical and NMR spectra of model diones[12] and was confirmed by synthesis.[13] The complete structure of the heme $d_1$ macrocycle is assigned as iron *cis*-1,3-bis(carbomethoxymethyl)-7-(carbomethoxyethenyl)-6-(carbomethoxyethyl)-1,3,5,8-tetramethyl-2,4-dioxoporphyrin.[13] Montforts et al.[14] have recently reported a new synthetic route to these macrocycles.

Although isobacteriochlorins (iBCs[11]) also have two adjacent saturated pyrrole rings, the two classes of macrocycle have little in common. The chemical reactivity of dione models differs from that of iBCs.[15-17] For example, reduction potentials of diones are only slightly above or are comparable with those of the parent porphyrins.[16] In contrast, it is much harder to oxidize a porphyrin than an iBC.[18] (Biological iBCs occur as the siroheme prosthetic macrocycle of assimilatory nitrite reductases.[19]) Furthermore, X-ray crystal structures of diones indicate only a very slight ruffling of the macrocycle,[14] with a general planarity and imposed rigidity, due to the double-bonded oxygens.[16a] In contrast, considerable $S_4$ ruffling is generally typical of iBCs.[16b] Indeed, data suggest that hydroporphyrin and oxoporphyrin complexes are distinct species.[18]

Resonance Raman (RR) spectroscopy is a method of spectral and structural analysis that can provide detailed insight into the

* To whom correspondence should be addressed.

(1) (a) Oregon Graduate Institute of Science and Technology. (b) Present address: Regional Sophisticated Instrumentation Center, Indian Institute of Technology, Madras 600036, India. (c) Kansas State University. (d) Michigan State University.

(2) (a) Iwasaki, H.; Matsubara, T. *J. Biochem. (Tokyo)* **1971**, *69*, 847-857. (b) Sawney, V.; Nicholas, D. J. D. *J. Gen. Microbiol.* **1978**, *106*, 119-128. (c) LeGall, J.; Payne, W. J.; Morgan, T. V.; DerVartanian, D. V. *Biochem. Biophys. Res. Commun.* **1979**, *87*, 355-362. (d) Wharton, D. C.; Wintraub, S. T. *Biochem. Biophys. Res. Commun.* **1980**, *97*, 236-242.

(3) (a) Greenwood, C. In *Metalloproteins*; Harrison, P. M., Ed.; Verlag Chemie: Weinheim, FRG, 1985; Part I, pp 43-77. (b) Kuronen, T.; Saraste, M.; Ellfolk, N. *Biochim. Biophys. Acta* **1975**, *393*, 48-54. (c) Horio, T.; Higashi, T.; Yamanaka, T.; Matsubara, H.; Okunuki, J. *J. Biol. Chem.* **1961**, *236*, 944-951.

(4) Kuronen, T.; Ellfolk, N. *Biochim. Biophys. Acta* **1972**, *275*, 308-318.

(5) (a) Gudat, J. C.; Singh, J.; Wharton, D. C. *Biochim. Biophys. Acta* **1976**, *157*, 423-430. (b) Parr, S. R.; Barber, D.; Greenwood, C.; Phillips, B. W.; Melling, J. *Biochem. J.* **1976**, *157*, 423-430.

(6) Lam, Y.; Nicholas, D. J. D. *Biochim. Biophys. Acta* **1969**, *180*, 459-472.

(7) Newton, N. *Biochim. Biophys. Acta* **1969**, *185*, 316-331.

(8) Timkovich, R.; Dhesi, R.; Martinkus, K. J.; Robinson, M. K.; Rea, T. M. *Arch. Biochem. Biophys.* **1982**, *215*, 47-58.

(9) (a) Yamanaka, T.; Okunuki, K. *Biochim. Biophys. Acta* **1963**, *67*, 407-416. (b) Timkovich, R.; Cork, M. S.; Taylor, P. V. *J. Biol. Chem.* **1984**, *259*, 1577-1585. (c) Timkovich, R.; Cork, M. S.; Taylor, P. V. *J. Biol. Chem.* **1984**, *259*, 15089-15093.

(10) Chang, C. K. *J. Biol. Chem.* **1985**, *260*, 9520-9522.

(11) Abbreviations used: dione, porphyrindione or dioxoporphyrin; iBC, isobacteriochlorin; SERRS, surface-enhanced resonance Raman scattering; OEP, octaethylporphyrin; MP, mesoporphyrin; Me, methyl; Et, ethyl; Ac, acetic acid methyl ester; Acr, acrylic acid methyl ester; Pro, propionic acid methyl ester; TME, tetramethyl ester; DME, dimethyl ester.

(12) (a) Chang, C. K.; Timkovich, R.; Wu, W. *Biochemistry* **1986**, *25*, 8447-8453. (b) Chang, C. K.; Sotiriou, C.; Wu, W. *J. Chem. Soc., Chem. Commun.* **1986**, 1213-1215.

(13) Wu, W.; Chang, C. K. *J. Am. Chem. Soc.* **1987**, *109*, 3149-3150.

(14) Montforts, F.-P.; Romanowski, F.; Bats, J. W. *Angew. Chem., Int. Ed. Engl.* **1989**, *28*, 480-483.

(15) Stolzenberg, A. M.; Strauss, S. H.; Holm, R. H. *J. Am. Chem. Soc.* **1981**, *103*, 4763-4778.

(16) (a) Chang, C. K.; Barkigia, K. M.; Hanson, L. K.; Fajer, J. *J. Am. Chem. Soc.* **1986**, *108*, 1352-1354. (b) Barkigia, K. M.; Fajer, J.; Chang, C. K.; Williams, G. J. B. *J. Am. Chem. Soc.* **1982**, *104*, 315-317.

(17) Chang, C. K.; Wu, W. *J. Org. Chem.* **1986**, *51*, 2134.

0002-7863/91/1513-5000$02.50/0 

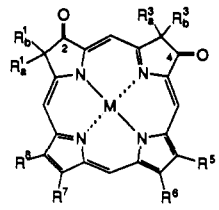

1 - 6

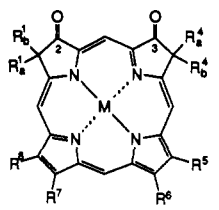

7 - 9

| Porphyrindiones[a] | $R^1$ | | $R^2$ | | $R^3$ | | $R^4$ | | $R^5$ | $R^6$ | $R^7$ | $R^8$ |
|---|---|---|---|---|---|---|---|---|---|---|---|---|
| | a | b | a | b | a | b | a | b | | | | |
| 1 Heme $d_1$ | Me | Ac | Oxo | - | Me | Ac | Oxo | - | Me | Pro | Acr | Me |
| 2 Cu-trans-$d_1$ TME | Me | Ac | Oxo | - | Me | Ac | Oxo | - | Me | Pro | Acr | Me |
| 3 Cu-cis-$d_1$ TME | Me | Ac | Oxo | - | Me | Ac | Oxo | - | Me | Pro | Acr | Me |
| 4 Cu-7-Acr-2,4-dione DME | Me | Et | Oxo | - | Me | Et | Oxo | - | Me | Pro | Acr | Me |
| 5 Cu-2,4-MPdione DME | Me | Et | Oxo | - | Me | Et | Oxo | - | Me | Pro | Pro | Me |
| 6 Cu-2,4-OEPdione | Et | Et | Oxo | - | Et | Et | Oxo | - | Et | Et | Et | Et |
| 7 Cu-7-Acr-2,3-dione DME | Me | Et | Oxo | - | Oxo | - | Me | Et | Me | Pro | Acr | Me |
| 8 Cu-2,3-MPdione DME | Me | Et | Oxo | - | Oxo | - | Me | Et | Me | Pro | Pro | Me |
| 9 Cu-2,3-OEPdione | Et | Et | Oxo | - | Oxo | - | Et | Et | Et | Et | Et | Et |

[a]Macrocycle number designations for substituent position (R') are according to the Fischer nomenclature system. M = iron for 1 and copper(II) for 2 - 9. The abbreviations used are defined in note 11.

**Figure 1.** Metalloporphyrindione with various peripheral substituents.

active-site structure and environment of heme proteins and enzymes.[20,21] Extension of RR spectroscopy to the study of hydroporphyrins has begun to prove very fruitful, with novel findings such as the unexpected sensitivity of chlorin RR spectra to macrocyclic deformation and even to pyrroline stereochemistry.[22] Cotton et al.[23] have reported the RR and SERRS[11] signatures of the *c* and $d_1$ chromophores from *Ps. aeruginosa* and *P. denitrificans*. Subsequently, Ching et al.[24] also examined the RR spectra of the *Ps. aeruginosa* enzyme. Most recently, a study of the copper(II)-metalated TME[11] of heme $d_1$ extracted from *Ps. aeruginosa* was reported, along with preliminary data for two dione model complexes.[25] However, no detailed analyses of spectral and structural properties of the dione macrocycle exist.

To explore the effects of each of the structural components of the $d_1$ macrocycle, we have examined the electronic absorption, Fourier transform infrared (FTIR), and RR spectra of eight different dione model complexes (Figure 1). This set of model compounds permits the systematic study of spectral and structural effects arising from (a) the relative stereochemistry of the acetates on the two pyrroline rings (**2** vs **3**); (b) acetate vs ethyl substituents (**2** and **3** vs **4**); (c) the acrylate moiety (**4** vs **5** and **7** vs **8**); (d) asymmetric vs symmetric patterns of substitution (**5** vs **6** and **8** vs **9**); and (e) the position of the oxo groups (**2–6** vs **7–9**). This work also includes study of the $^{15}N_4$- and meso-$d_4$-substituted complexes of Cu-2,4-OEPdione (**6**) and Cu-2,3-OEPdione (**9**). Additional goals of this study were to identify correlations between the well-known vibrational modes of porphyrins and those of diones and to determine specific spectral properties diagnostic for diones vs porphyrins, chlorins, and iBCs.

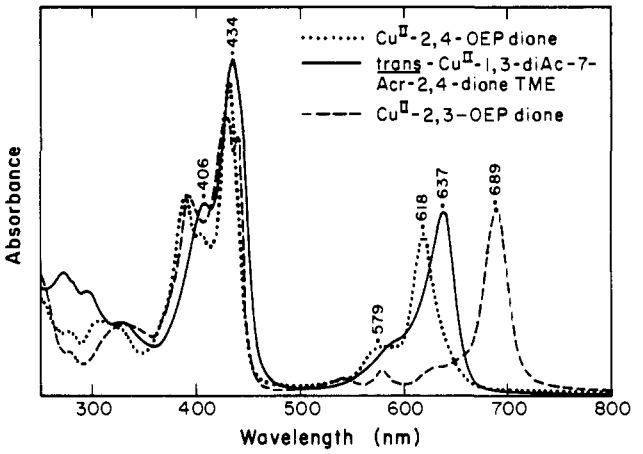


**Figure 2.** Electronic absorption spectra of the copper diones: solid line, *trans*-Cu-$d_1$-TME (**2**); dotted line, Cu-2,4-OEPdione (**6**); dashed line, Cu-2,3-OEPdione (**9**). Peak positions listed in Table I.

**Table I.** Absorption Maxima (nm) for Metallodiones[a]

| no. | compound | B | | $Q_y(0,1)$ | $Q_y(0,0)$ |
|---|---|---|---|---|---|
| | 2,4-Diones | | | | |
| 2 | *trans*-Cu-$d_1$-TME | 406 | 434 | 589 | 637 |
| 3 | *cis*-Cu-$d_1$-TME | 409 | 433 | 594 | 638 |
| 4 | Cu-7-Acr-2,4-dione-DME | 407 | 434 | 591 | 641 |
| 5 | Cu-2,4-MPdione-DME | 390 | 403 | 429 | 578 | 618 |
| 6 | Cu-2,4-OEPdione | 389 | 404 | 430 | 579 | 618 |
| | 2,3-Diones | | | | |
| 7 | Cu-7-Acr-2,3-dione-DME | 412 | 448 | 633 | 683 |
| 8 | Cu-2,3-MPdione-DME | 396 | 422 | 438 | 627 | 684 |
| 9 | Cu-2,3-OEPdione | 393 | 427 | 438 | 630 | 689 |

[a]Samples in $CH_2Cl_2$.

Key findings: (1) Not only conjugated but also nonconjugated peripheral substituents affect the RR and FTIR spectral properties of diones. (2) Dione "marker bands" include not only the expected $\nu$(C=O) modes but also a $^{15}N_4$-sensitive vibrational mode in the ~1340–1350-cm$^{-1}$ RR region. (3) The novel meso-$d_4$ sensitivity of the latter feature clearly indicates that the normal-mode composition of diones differs from that of porphyrins, as well as from chlorins and iBCs. These data should also aid in more detailed analyses of correlations between structure and function for the heme $d_1$ macrocycle of dissimilatory nitrite reductases.

## Experimental Section

Free-base model dione complexes were synthesized as described by Chang[13,25] and were examined for purity by $^1$H NMR spectroscopy. The $^{15}N_4$- and meso-$d_4$-substituted derivatives of the 2,3- and 2,4-octaethylporphyrindiones (OEPdiones; Figure 1) were prepared from [$^{15}N_4$]OEP (98% $^{15}$N) and *meso*-OEP-$d_4$ (95% *d*), respectively, according to the stepwise osmation and rearrangement procedure.[12b] Insertion of copper(II) in the dione model complexes was accomplished by heating a $CHCl_3$ solution of the compound with copper(II) acetate in $CH_3OH$.[12b]

Electronic absorption spectra of the copper dione samples in $CH_2Cl_2$ solution were obtained on a Perkin-Elmer Lambda-9 spectrophotometer with a spectral bandwidth of 1.0 nm. FTIR spectra were obtained from KBr pellets (~1:300 ratio of compound hydroporphyrin to KBr) on a Perkin-Elmer 1800 spectrometer. Resonance Raman spectra were obtained from solid-state samples (1:300 in a KBr matrix), placed in a grooved sample holder that was spun during laser irradiation. Alternatively, ~1 mg/mL $CH_2Cl_2$ solution samples, sealed in standard melting point capillaries, were placed in a copper cold finger held in a bath of ice water during laser irradiation. Surprisingly, little or no difference in RR spectral frequencies or relative intensities was observed between solution- and solid-state dione complexes. However, solution samples were more difficult to study given the fluorescence from trace free-base diones and a slight photolability.

Variable-wavelength excitation was provided with a Spectra-Physics Model 2025-11 Krypton ion and a Coherent Innova 90 Argon ion laser with a CR 599 dye laser. Resonance Raman spectra were obtained with computer-controlled Dilor Z24 and Jarrell-Ash Raman spectrometers.

(18) (a) Chang, C. K.; Hanson, L. K.; Richardson, P. R.; Young, R.; Fajer, J. *Proc. Natl. Acad. Sci. U.S.A.* **1981**, *78*, 2652–2656. (b) Stolzenberg, A. M.; Glazer, P. A.; Foxman, B. M. *Inorg. Chem.* **1986**, *25*, 983–991.
(19) Siegel, L. M.; Ruger, D. C.; Barber, M. J.; Krueger, R. J.; Orme-Johnson, N. R.; Orme-Johnson, W. H. *J. Biol. Chem.* **1982**, *257*, 6343–6350.
(20) Felton, R. H.; Yu, N.-T. In *The Porphyrins*; Dolphin, D., Ed.; Academic Press: New York, 1978; Vol. III Chapter 8, pp 347–393.
(21) Spiro, T. G. In *Iron Porphyrins*, Part II; Lever, A. B. P., Gray, H. B., Eds.; Addison-Wesley: Reading, MA, 1983; Chapter 3, pp 91–159.
(22) Andersson, L. A.; Loehr, T. M.; Stershic, M. T.; Stolzenberg, A. M. *Inorg. Chem.* **1990**, *29*, 2278–2285 and references therein.
(23) Cotton, T. M.; Timkovich, R.; Cork, M. S. *FEBS Lett.* **1981**, *133*, 39–44.
(24) Ching, Y.; Ondrias, M. R.; Rousseau, D. L.; Muhoberac, B. B.; Wharton, D. C. *FEBS Lett.* **1982**, *138*, 239–244.
(25) Andersson, L. A.; Loehr, T. M.; Wu, W.; Chang, C. K.; Timkovich, R. *FEBS* Lett. **1990**, *267*, 285–288.

**Table II.** Structurally Sensitive Vibrational Frequencies for Copper Diones[a]

| | FTIR | | | Resonance Raman | | | | |
|---|---|---|---|---|---|---|---|---|
| | ν(C=O)[b] | ν(C=O)[c] | ν(C=C)[d] | ν(C=O)[c] | I[e] | II | III | IV[f] |
| | | | | 2,4-Diones | | | | |
| 1[g] | | | | 1721 | 1647 | 1536 | 1509? | 1339 |
| 2 | 1738 | 1724 | 1628 | 1723 | 1648 | 1538 | 1511 | 1340 |
| 3 | 1738 | 1721 | 1625 | 1721 | 1648 | 1538 | 1512 | 1341 |
| 4 | 1738 | 1718 | 1627 | 1721 | 1648 | 1535 | 1511 | 1342 |
| 5 | 1738 | 1714 | n.o.[h] | 1715 | 1644 | n.o. | 1513 | 1340 |
| 6 | n.o. | 1717, 1701 | n.o. | 1718, 1701 | 1644 | n.o. | 1511 | 1337 |
| | | | | 2,3-Diones | | | | |
| 7 | 1738 | 1717 | 1623 | 1718 | 1645 | 1535 | 1518 | 1341 |
| 8 | 1736 | 1712 | n.o. | 1709 | 1642 | n.o. | 1519 | 1342 |
| 9 | n.o. | 1708, 1696 | n.o. | 1706, 1698 | 1642 | n.o. | 1520 | 1346 |

[a] Frequencies in $cm^{-1}$. [b] Ester carbonyl. [c] Oxo carbonyl. [d] Acrylate double bond. [e] The related porphyrin mode is most likely $\nu_{10}$. [f] The related porphyrin mode is most likely $\nu_{41a}$. [g] In this table, **1** is the Cu(II)-metalated heme $d_1$.[25] [h] Not observed.

The Raman instruments were calibrated against indene frequencies.

## Results and Discussion

**A. Electronic Spectra.** Upon saturation of one or more porphyrin pyrrole rings to yield a hydroporphyrin, there are dramatic changes in the electronic absorption spectra. For a chlorin, the saturation of one pyrrole ring leads to the characteristic strong band at ~600 nm [$Q_y(0,0)$]. For an iBC, the saturation of two adjacent pyrrole rings of the macrocycle also leads to altered spectral properties vs those of the "parent" porphyrin.[15]

The electronic absorption spectra of dione models **2**, **6**, and **9** are shown in Figure 2. Electronic transitions for these complexes and for the other copper dione model complexes are listed in Table I. Several features stand out as notable. First of all, the electronic spectra of Cu-2,3-OEPdione (**9**) are very different from those of Cu-2,4-OEPdione (**6**). For example, the $Q(0,0)$ band of **9** is at 689 nm, vs 618 nm for the 2,4-OEPdione (**6**). Thus, it is the $Q_y(0,1)$ band of the Cu-2,3-OEPdione that is close in wavelength to the $Q_y(0,0)$ band of the Cu-2,4-OEPdione. This wide spectral variance is typical for all the 2,4-diones (**2–6**) vs 2,3-diones (**7–9**), as shown in Table I. Indeed, the absorption spectra of the copper 2,3-diones are most similar to those of bacteriochlorins, which also have a strong band in the far-red region of the absorption spectra.[30] These data illustrate the strong effect that the oxo groups have on the electronic absorption spectra.

An asymmetric vs symmetric pattern of peripheral substituents has no major effect on the electronic absorption spectral properties of the 2,4-dione models **5** vs **6** (only 1-nm shifts for the transitions). However, in the case of the symmetrical 2,3-diones, shifts up to 5 nm occur, demonstrating a stronger effect from the loss of overall macrocyclic symmetry (**8** vs **9**, Table I). Addition of the 7-acrylate substituent has a dramatic effect on the spectra: For both the 2,4- and 2,3-dione model complexes, the three-banded Soret becomes two-banded. Furthermore, there are also spectral shifts. For example, an ~20-nm red shift of $Q_y(0,0)$ occurs for 2,4-dione model **4** vs **5**, with an ~10-nm red shift of the $Q_y(0,1)$ band, but no additional (major) changes in the Soret region. In contrast, for the 2,3-dione models, there is little shifting of $Q_y(0,0)$ or $Q_y(0,1)$, but both the Soret bands are shifted from those of the models without the 7-acrylate group. These differences between the 2,4- and 2,3-diones are an intriguing illustration of the effect of a conjugated substituent on the molecular orbitals.

Finally, as shown in Table I, there are minor red shifts between the absorption bands of the *cis*- vs *trans*-Cu-$d_1$-TME models. Similar red shifts occur between the *cis*- vs *trans*-nickel(II) dioxoporphyrins of Montforts et al.[14] Indeed, these data also parallel the bathochromic shifts we observed between *cis*- and *trans*-metallooctaethylchlorin models.[22] Thus, there now appears to be sufficient precedent to make the generalization that the electronic absorption spectra of *cis*-hydroporphyrins can be expected to be red shifted with respect to those of *trans*-hydroporphyrins.

**B. Symmetry Reduction.** Porphyrins have effective $D_{4h}$ symmetry and are essentially planar macrocycles whereas chlorins are $S_4$ ruffled and can be extremely nonplanar. Crystal structures of both iBCs and diones also indicate a lowering of symmetry from $D_{4h}$ to $C_2$.[16,26] This symmetry reduction relative to porphyrins means that the mutual exclusion principle is no longer valid. Thus, IR modes become Raman allowed and vice versa, leading to an increase in the total number of active vibrational modes in both the FTIR and RR spectra.

A significant aspect of the vibrational properties of tetrahydroporphyrins with adjacent saturated rings (diones and iBCs) derives from the 45° rotation of the $C_2$ symmetry axis relative to that of chlorins.[25,27–30] This rotation results in a reversal of the polarization properties observed in the RR spectra for the porphyrin-derived $B_{1g}$ and $B_{2g}$ modes. That is, both the $B_{1g}$ and $B_{2g}$ modes are depolarized in RR spectra of porphyrins. However, they are, respectively, polarized and depolarized for chlorins but are depolarized and polarized for both diones and iBCs.

**C. Effects of Peripheral Substitution. 1. Carbonyl Modes.** As stated previously,[25] "a porphyrindione is not simply an iBC with oxo substituents". The conjugated oxo groups of the diones confer a surprising rigidity to the macrocycles, relative to other hydroporphyrins such as iBCs.[14,16a,b,18] This is perhaps best exemplified by the fact that RR data for the porphyrindiones were very similar between solution- and solid-state samples, with respect to *both* frequencies *and* patterns of relative intensity.

As shown in Figure 3 and Table II, the ν(C=O) modes of the copper dione model complexes are surprisingly sensitive to structural variations at the periphery of the macrocycles. We previously suggested that the ν(C=O) modes of the two oxo groups of Cu-$d_1$ were accidentally degenerate.[25] For dione models **2–5**, **7**, and **8**, neither the FTIR spectra nor the RR spectra display separate $\nu_{oxo}$(C=O) modes. The $\nu_{oxo}$(C=O) modes of **2–5**, **7**, and **8** need not necessarily be accidentally degenerate to display the observed lack of splitting. Coupling of the two oxo carbonyl modes, with one of the two being strong and the other weak, is perhaps more likely. However, for the OEPdione complexes **6** and **9**, both having the symmetrical octaethyl substituent pattern, there are clearly two resolved ν(C=O) bands, although their frequencies differ. The frequencies for complex **9** are the lowest of any of the model diones studied (Table II). As expected, the $\nu_{oxo}$(C=O) modes for the OEPdiones are not very sensitive to either $^{15}N_4$ or meso-$d_4$ substitution (Table III).

The $\nu_{oxo}$(C=O) frequency of the dione models decreases slightly, but consistently, in response to modification of the peripheral substituents, whether conjugated or nonconjugated. For example, the $\nu_{oxo}$(C=O) FTIR mode of **2** is at 1724 $cm^{-1}$, vs 1721 $cm^{-1}$ for **3**. This shift is admittedly minor. Nonetheless, it is

(26) Suh, M. P.; Swepston, P. N.; Ibers, J. A. *J. Am. Chem. Soc.* **1984**, *106*, 5164–5171.
(27) Li, X.-Y.; Czernuszewicz, R. S.; Kincaid, J. R.; Stein, P.; Spiro, T. G. *J. Am. Chem. Soc.* **1990**, *94*, 47–61.
(28) Andersson, L. A.; Loehr, T. M.; Thompson, R. G.; Strauss, S. H. *Inorg. Chem.* **1990**, *29*, 2142–2147.
(29) Andersson, L. A.; Mylrajan, M.; Loehr, T. M.; Sullivan E. P., Jr.; Strauss, S. H. *New J. Chem.* **1991**, in press.
(30) (a) Scheer, H. In *The Porphyrins*; Dolphin, D., Ed.; Academic Press: New York, 1978; Vol. II, pp 1–44. (b) Scheer, H.; Inhoffen, H. H. In *The Porphyrins*; Dolphin, D., Ed.; Academic Press: New York, 1978; Vol. II, pp 45–90.

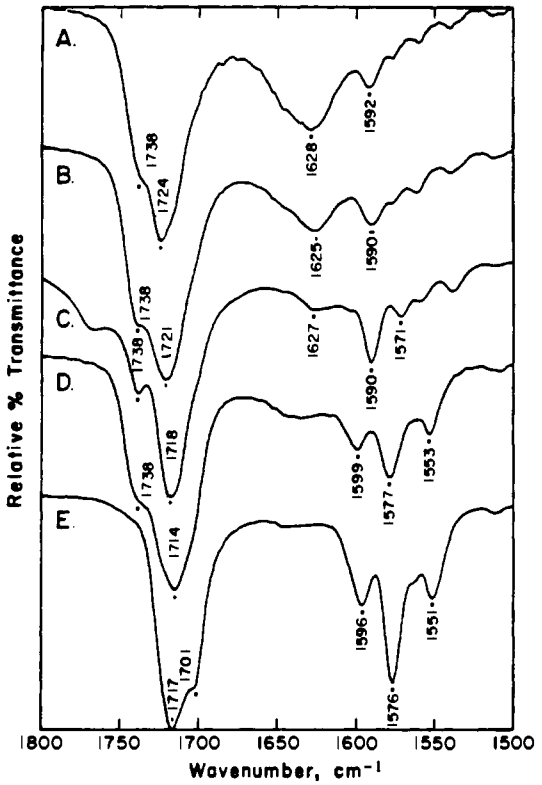


**Figure 3.** Carbonyl region FTIR spectra of copper-2,4-diones: A, *trans*-Cu-$d_1$-TME (**2**); B, *cis*-Cu-$d_1$-TME (**3**); C, Cu-7-Acr-2,4-dione-DME (**4**); D, Cu-2,4-MPdione-DME (**5**); E, Cu-2,4-OEPdione (**6**).

intriguing that alteration of the relative stereochemistry of the acetate groups on the two *different* pyrroline rings should have *any* effect on the $\nu_{oxo}$(C=O) frequencies. Indeed, this observation is reminiscent of the surprisingly strong effect that the stereochemistry of pyrroline substituents has on the RR and FTIR spectra of *cis*- and *trans*-metallooctaethylchlorins.[22] Substituent-induced spectral anomalies have also been noted by us for other chlorins.[31]

Overall, the carbonyl region FTIR spectra of dione models **4** and **7** (or models **5** and **8**) are quite similar. In fact, the vibrational spectra of the asymmetrically substituted 2,4- vs 2,3-diones exhibit considerably less variance than do their absorption spectra.

Some of the dione model complexes also have ester and acetate carbonyl groups. The 1738-cm$^{-1}$ $\nu$(C=O) band in the FTIR spectra arises from the $C_7$ and $C_8$ esters of model diones **2–5**, **7**, and **8**, as well as from the $C_{1b}$ and $C_{3b}$ acetate esters of dione models **2** and **3** (Figure 3). The $\nu$(C=O) frequency of the esters is essentially identical across the set of models studied, with the exception of a slight downshift for model **8** (Table II). The weak and broad shoulder at ~1650 cm$^{-1}$ in the FTIR spectra of *trans*- and *cis*-Cu-$d_1$ (**2** and **3**) may be due to $\nu$(C=O) of the $C_{1b}$ and $C_{3b}$ acetyl groups. Neither of these two $\nu$(C=O) features is observed in the RR spectra.

**2. Other Vibrational Modes.** RR bands that are also sensitive to the change in peripheral substituents across the set of model diones are listed in Table II. All of the models that have the 7-acrylate moiety (**2–4**, **7**) display two bands in the 1500–1550-cm$^{-1}$ region (Figure 4). The second band, when present, is found at ~1535–1540 cm$^{-1}$. However, when the 7-acrylate group is absent, there is only a single band in this region. Given the apparent correlation of the ~1535–1540-cm$^{-1}$ feature with the presence of 7-acrylate substituent, the absence of a frequency shift between 2,3-diones and 2,4-diones suggests that the vibrational mode involved is isolated from oxo group effects.

The band frequencies in this region also vary with the pattern of peripheral substituents. For example, the 2,3-dione models have an RR band at ~1520 cm$^{-1}$ vs an ~1510-cm$^{-1}$ band for the 2,4-diones (Table II; Figure 4 part A vs parts B and C). Comparison of RR data for Cu-7-Acr-2,3-dione (**7**) and Cu-7-Acr-2,4-dione-DME (**4**) indicates lower frequencies for many RR bands of the 2,3-dione, e.g., 1644 vs 1648 cm$^{-1}$ and 1603 vs 1606 cm$^{-1}$ for models **7** vs **4**, respectively (Table III; Figure 3). The patterns of relative intensity, and thus the excited states of the two macrocycles, differ also, as seen with 457.9-nm excitation.

**Table III.** RR Frequency Correlations for Cu-2,4- and -2,3-OEPdiones[a]

| Cu-2,4-OEPdione | | | Cu-2,3-OEPdione | | | | |
|---|---|---|---|---|---|---|---|
| $\nu$ | $\Delta^{15}N_4$ | $\Delta d_4$ | $\nu$ | $\Delta^{15}N_4$ | $\Delta d_4$ | $\rho^b$ | correlation[c] |
| 1718 | 0 | 0 | 1705 | 2 | 2 | p | $\nu$(C=O) |
| 1701 | 0 | 0 | 1694 | 0 | 0 | p | |
| 1644 | 0 | 9 | 1642 | 0 | 12 | dp | $\nu_{10}$ |
| 1603 | 0 | 8 | | | | p | $\nu_{37}$ |
| 1595 | 0 | 9 | | | | | $\nu_2$ |
| 1576 | 1 | 10 | 1570 | 0 | 8 | dp | $\nu_{19}$ |
| 1561 | 1 | 8 | | | | p | |
| 1555 | 0 | 11 | 1556 | 0 | 14 | p | $\nu_{11}$ |
| 1511 | 1 | 10 | 1520 | 0 | 8 | p | $\nu_3$ |
| 1482 | 1 | 14 | 1486 | 1 | 10 | p | $\nu_{28}$ |
| 1475 | 5 | 7 | 1466 | 0 | 13 | p | |
| 1462 | 1 | 1 | (1457) | 1 | 1 | | |
| 1400 | 1 | 0 | 1392 | 0 | 0 | p | $\nu_{29}$ |
| 1391 | 6 | 25 | 1386 | 5 | 38 | p | $\nu_4$, $C_aN$ and $C_aC_m$ |
| 1375 | 0 | 16 | | | | | |
| 1361 | 0 | 5 | | | | p | |
| 1337 | 5 | 9 | 1346 | 8 | 12 | p | $\nu_{41a}$, $C_aN$ and $C_aC_m$ |
| 1319 | 4 | | 1324 | 6 | | dp | $\nu_{12}$ |
| 1302 | 3 | | 1310 | 3 | | | |
| 1265 | 1 | 5 | 1272 | 2 | | p | |
| 1244 | 3 | | 1239 | 4 | | p | |
| 1227 | 3 | | 1227 | 5 | 1 | | |
| 1165 | 6 | 9 | 1168 | 5 | 14 | dp | |
| 1144 | 5 | 4 | 1137 | 6 | 0 | | |
| 1119 | 6 | 8 | 1115 | 16 | 11 | dp | |
| 1021 | 3 | 0 | 1023 | 2 | 0 | p | $\nu(C_1C_2)$ |
| 1003 | 8 | 7 | 992 | 4 | 6 | | |
| 961 | 4 | 4 | 958 | 2 | 3 | | |
| 917 | 4 | 10 | 911 | | | p | |
| 800 | 5 | 7 | 800 | | | | $\nu_6$ |
| 773 | 2 | 5 | 775 | | | | |
| 750 | 1 | 66 | 753 | 3 | 77 | dp | $\nu_{15}$ |
| 707 | 7 | 12 | 705 | 5 | 5 | dp | |
| 684 | 1 | 18 | 673 | 0 | | | |
| 525 | 2 | 4 | 528 | 3 | 5 | dp | |
| 338 | 1 | 0 | 341 | 0 | 0 | p | $\nu_8$ |
| 268 | 1 | 1 | 260 | 0 | 0 | p | $\nu_9$ |

[a] Frequencies in cm$^{-1}$; FTIR bands in parentheses. [b] Depolarization ratios = $\rho$;[34] p = polarized; dp = depolarized. [c] Correlation with related porphyrin mode made on the basis of comparable isotopic shifts and previous studies.[27,32,33]

**D. Dione "Marker Band(s)".** An obvious marker for the dione macrocycle is the $\nu$(C=O) band, discussed in detail above. However, a second feature in the RR spectra is specific and diagnostic for the dione macrocycle. This is the strong band at 1341 cm$^{-1}$ in the RR spectra of Cu-7-Acr-2,3-dione-DME (Figure 4A). This feature is present in RR spectra of all the dione models and is (most) intense with Soret and/or near-Soret excitation wavelengths. For example, the spectrum of *trans*-Cu-$d_1$-TME, a close structural analogue of heme $d_1$, has a strong 1340-cm$^{-1}$ band (Figure 4C). A similar band near 1350 cm$^{-1}$ is also present in RR spectra of heme $d_1$.[23,24]

The ~1340-cm$^{-1}$ RR band is $^{15}N_4$-isotope sensitive for both the Cu-2,4-OEPdione and Cu-2,3-OEPdione models (Figures 5–7; Table III). The downshift observed upon $^{15}N_4$ substitution is similar to that observed for the $\nu_4$ band and to that predicted for the $\nu_{12}$ band in the "oxidation-state marker region" of metalloporphyrins. This is exemplified for Ni$^{II}$OEP, as reported by Abe et al.,[32] and more recently by Li et al.[27]

(31) Andersson, L. A.; Sotiriou, C.; Chang, C. K.; Loehr, T. M. *J. Am. Chem. Soc.* **1987**, *109*, 258–264.

(32) Abe, M.; Kitagawa, T.; Kyogoku, Y. *J. Chem. Phys.* **1978**, *69*, 4526–4534.

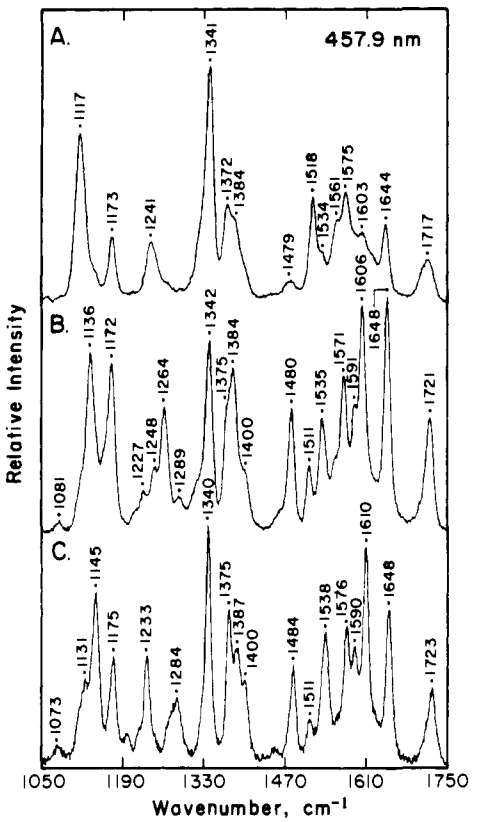


**Figure 4.** High-frequency, 457.9-nm excitation RR spectra of copper diones: A, Cu-7-Acr-2,3-dione-DME (**7**); B, Cu-7-Acr-2,4-dione-DME (**4**); C, *trans*-Cu-$d_1$-TME (**2**). Experimental conditions: sample in ~1:300 KBr matrix in spinning cell; 30-mW laser power; scan rate, 1 $cm^{-1}$/step (Dilor) or 1 $cm^{-1}$/s (Jarrell-Ash); slit width, 5 $cm^{-1}$; 5-s accumulation; average of two to five scans.

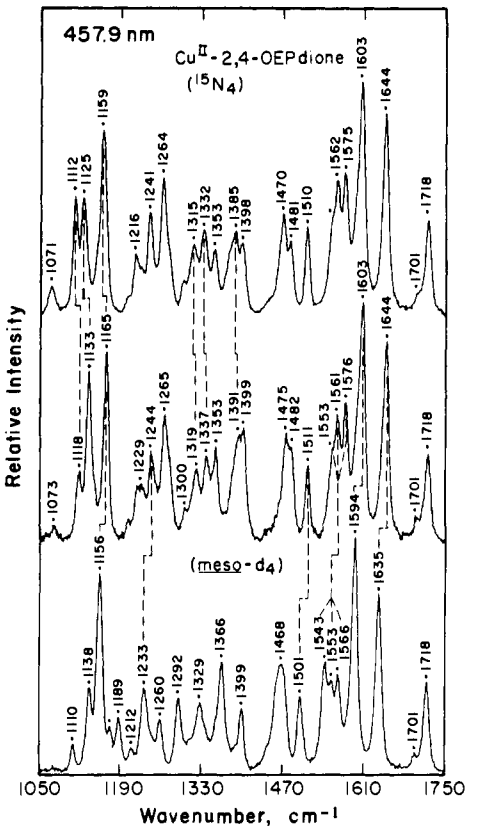


**Figure 5.** High-frequency, 457.9-nm excitation resonance Raman spectra of Cu-2,4-OEPdione (**6**) (center) and its $^{15}N_4$- (top) and meso-$d_4$- (bottom) substituted isomers. Conditions: as in Figure 4. The RR spectrum of **6** in $CH_2Cl_2$ solution is virtually identical with that of the solid-state sample, with respect to both peak positions and relative intensities.

A second polarized, $^{15}N_4$-sensitive feature appears at ~1385-1391 $cm^{-1}$ in spectra of the 2,3- and 2,4-OEPdiones (Table III; Figures 5–7). If we assume that the latter correlates approximately with the $\nu_4$ ($A_{1g}$) band of porphyrins, then the former, characteristic dione band at ~1340 $cm^{-1}$ is likely to correlate with the $\nu_{41}$ ($E_u$) band as predicted by Abe et al.[32] It cannot correlate with, or arise from, the $\nu_{12}$ ($B_{1g}$) mode of the porphyrin "parent", because the latter mode is expected to be depolarized in RR spectra of diones on the basis of symmetry arguments discussed above.

The ~1340-$cm^{-1}$ RR band of the dione models is surprisingly intense. A feature having this intensity is not routinely observed in RR spectra of porphyrins, chlorins, or isobacteriochlorins. Furthermore, no such feature at this approximate frequency and having $^{15}N_4$ sensitivity is present in RR spectra for the latter macrocycles. Thus, the ~1341-$cm^{-1}$ feature of diones is particular to, and diagnostic for, the dione macrocycle, regardless of the pattern of 2,4- or 2,3-substitution.

The RR data clearly and unequivocally indicate that the normal-mode composition of a dione is distinct from that of the parent porphyrin, at the least with respect to the ~1340–1345-$cm^{-1}$ vibrational feature. This can readily be observed from Table III, where we show that the ~1340-$cm^{-1}$, $\nu_{41}$-related mode of the dione is also sensitive to meso-$d_4$ substitution. However, because the 9–12-$cm^{-1}$ shifts observed for this RR band of the 2,4- and 2,3-OEPdiones are far greater than that calculated or observed for the $\nu_{41}$ feature of Ni$^{II}$OEP,[32] the mode composition for the two types of macrocycle cannot be identical.

**E. Comparison of Cu-2,4- and -2,3-OEPdiones and Their $^{15}N_4$ and Meso-$d_4$ Isomers.** High-frequency bands >1100 $cm^{-1}$ for Cu-2,4-OEPdione are shown in Figures 5 and 6, along with data for its $^{15}N_4$ and meso-$d_4$ isotopomers. Similar data for the Cu-2,3-OEPdione complex are shown in Figure 7. The frequencies and proposed assignments, or porphyrin mode correlations, for both model complexes are listed in Table III.

Resonance Raman spectra of Cu-2,4-OEPdione (**6**) are more complex than those of Cu-2,3-OEPdione (**9**), as shown in Figures 6 and 7 and Table III. This is because the asymmetric disposition of the two oxo groups on the Cu-2,4-OEPdione macrocycle lowers the effective symmetry. Thus, one expects to observe more vibrational bands in spectra of Cu-2,4-OEPdione.

In the $\nu_4$ marker region, as many as six bands are present in the RR spectra of Cu-2,4-OEPdione, as seen at 1337, 1353, 1361, 1375, 1391, and 1399 $cm^{-1}$. In contrast, Cu-2,3-OEPdione has only two distinct bands in this interval: the characteristic ~1345-$cm^{-1}$ band and another at 1386 $cm^{-1}$. The strong ~1345-$cm^{-1}$ band of Cu-2,3-OEPdione is fairly weak in the RR spectra of Cu-2,4-OEPdione. The latter complex is thus anomalous with respect to all other model diones studied here (**2–5**, **7–9**). The prominent band at 1345 $cm^{-1}$ in Cu-2,3-OEPdione (647.1-nm excitation) is sensitive to both $^{15}N_4$ and meso-$d_4$ substitution and is polarized. The band at 1386 $cm^{-1}$ also shows a 5-$cm^{-1}$ downshift with $^{15}N_4$ substitution, indicating $C_aN$ mode contributions for both the ~1340- and 1386-$cm^{-1}$ bands.

The RR bands of Cu-2,4-OEPdione at 1118, 1133, 1144, and 1165 $cm^{-1}$ shift with $^{15}N_4$ substitution, demonstrating $C_aN$ contributions to their normal modes. Normal-coordinate calculations for porphyrins also indicate large contributions to $C_aN$ modes in this region.[27,32,33] Bands at 1227 $cm^{-1}$ in the RR spectra of both

(33) Boldt, N. J.; Donohoe, R. J.; Birge, R. R.; Bocian, D. F. *J. Am. Chem. Soc.* **1987**, *109*, 2284–2298.

(34) As discussed previously,[35] we have used an operational definition of $\rho$ <0.5 to assign polarized modes. It is known that depolarized modes can have $\rho \simeq 0.6$–0.7, with Soret and near-Soret excitation, due to polarization dispersion.[21] For low-symmetry macrocycles such as the diones, considerable overlap of the large number of Raman-allowed bands (virtually *all* vibrational modes) can occur, causing precise measurement of depolarization ratios to be more difficult.

(35) Andersson, L. A.; Loehr, T. M.; Sotiriou, C.; Wu, W.; Chang, C. K. *J. Am. Chem. Soc.* **1986**, *108*, 2908–2916.

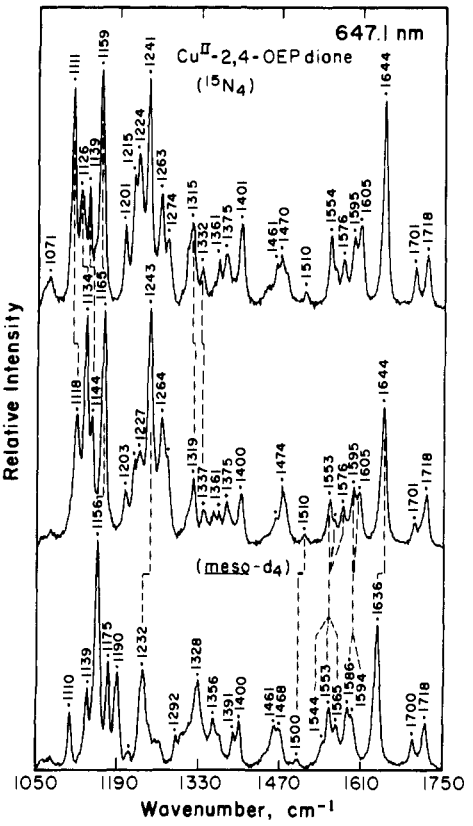


**Figure 6.** High-frequency, 647.1-nm excitation resonance Raman spectra of Cu-2,4-OEPdione (**6**) (center) and its $^{15}N_4$- (top) and meso-$d_4$- (bottom) substituted isomers. Conditions: laser power, 50 mW; other conditions, as in Figure 4.

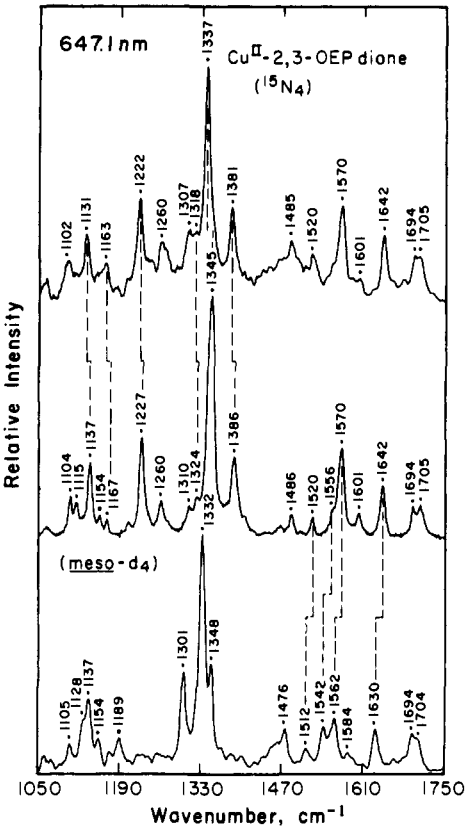


**Figure 7.** High-frequency, 647.1-nm excitation resonance Raman spectra of Cu-2,3-OEPdione (**9**) (center) and its $^{15}N_4$- (top) and meso-$d_4$- (bottom) substituted isomers. Conditions: laser power, 50 mW; other conditions, as in Figure 4.

Cu-2,3-OEPdione and Cu-2,4-OEPdione are likely to have $C_mH$ mode contributions given the large shifts upon meso-$d_4$ substitution. The 1021- and 1023-cm$^{-1}$ RR bands of Cu-2,4- and -2,3-OEPdiones did not shift significantly with $^{15}N_4$ and/or meso-$d_4$ substitution and are likely to be ethyl modes (Table III).

The four prominent RR bands of Cu-2,3-OEPdione at 1520, 1570, 1601, and 1642 cm$^{-1}$ are insensitive to $^{15}N_4$ substitution, but show 8–17-cm$^{-1}$ shifts upon meso-$d_4$ substitution (Figure 7). The 12-cm$^{-1}$ $d_4$ shift of the band at 1642 cm$^{-1}$ is similar to that observed for the $\nu_{10}$ mode of porphyrins.[33] The "$\nu_{10}$" mode of Cu-2,3-OEPdione is depolarized, as predicted on the basis of symmetry. Thus, for the dione (as for iBC's[33]), "$\nu_{10}$" is depolarized, whereas the analogous band of chlorins is polarized. $C_aC_m$ modes of porphyrins have meso-$d_4$ shifts, whereas $C_bC_b$ modes, such as $\nu_2$ and $\nu_{11}$, have no meso-$d_4$ shifts.[27,32] However, in the case of diones, *all* the modes above 1500 cm$^{-1}$ in the RR spectra are meso-$d_4$ sensitive, again indicating a mixing of normal modes.

### Biological Relevance

Model diones with 2,3-oxo groups are spectrally distinct from model and/or biological 2,4-substituted diones. This is perhaps most obvious in the elctronic absorption spectra, but may also be observed from the RR and FTIR data. As shown here, the spectra of model 2,4-substituted diones have bands at ~1720 cm$^{-1}$ assignable to $\nu$(C=O) of the keto groups. The separate $\nu$(C=O) features of the 2- and 4-oxo groups are likely to be coupled, or possibly accidentally degenerate.[25] However, there are two distinct $\nu$(C=O) bands in the case of OEPdiones. A slight sensitivity of the $\nu$(C=O) frequency to the peripheral substituents is observed. Resonance Raman spectra of the cytochrome $cd_1$ oxidase from *Ps. aeruginosa* have bands at ~1726 cm$^{-1}$.[23,24] Thus, $\nu$(C=O) frequencies agree well for in vivo heme $d_1$ and those models with a similar pattern of peripheral substituents (compare **1** and **2–4**, Table II).

The RR spectra have a unique $\nu_4$ band in the 1340–1350-cm$^{-1}$ region that is polarized, strong, and both $^{15}N_4$ and meso-$d_4$ sensitive. The strong band is also clearly present in RR spectra of the cytochrome $cd_1$ oxidase as well as in RR spectra of the tetracoordinate copper(II)-metalated TME of extracted heme $d_1$.[25] In contrast, bands in this region are generally absent from RR spectra of porphyrins, chlorins, and isobacteriochlorins (or are very weak). Thus, the presence of a strong, polarized, $^{15}N_4$-sensitive band at ~1340 cm$^{-1}$ appears diagnostic for both model and biological dione macrocycles.

Finally, those models bearing all the structural features of the in vivo heme $d_1$ display a spectral pattern closely analogous to that of $d_1$. Each incremental change in structure, from removal of the acrylate moiety to substitution of ethyls for acetates, etc., results progressively in a loss of spectral correspondence. Although the precise functional significance of each substituent of heme $d_1$ is not yet known, this study provides a foundation for further exploration of diones in dissimilatory nitrite reductases.

**Acknowledgment.** We thank Ms. Kaitlin Grammer for expert technical assistance. We also thank the reviewers for their helpful comments. This work was supported by the National Institutes of Health (Grants GM 34468 to T.M.L, L.A.A, and C.K.C). The support of the NIH is further acknowledged for its Biomedical Research Support Grant (S07 RR 07184) program, used toward the purchase of research instrumentation. This is Contribution No. 91-268-J from the Kansas Agricultural Experiment Station. C.K.C. thanks Dr. James Fee and the NIH (Grant RR02231)–USDOE/OHER Stable Isotope Program at Los Alamos.